Glacial geomorphology and cosmogenic [10]Be and [26]Al exposure ages in the northern Dufek Massif, Weddell Sea embayment, Antarctica

Dominic A. Hodgson, Michael J. Bentley, Christoph Schnabel, Andreas Cziferszky, Peter Fretwell, Peter Convey and Sheng Xu

How to cite this article:
Dominic A. Hodgson, Michael J. Bentley, Christoph Schnabel, Andreas Cziferszky, Peter Fretwell, Peter Convey and Sheng Xu (2012). Glacial geomorphology and cosmogenic [10]Be and [26]Al exposure ages in the northern Dufek Massif, Weddell Sea embayment, Antarctica. Antarctic Science,24, pp 377-394 doi:10.1017/S0954102012000016

Request Permissions : Click here

Glacial geomorphology and cosmogenic [10]Be and [26]Al exposure ages in the northern Dufek Massif, Weddell Sea embayment, Antarctica

DOMINIC A. HODGSON[1], MICHAEL J. BENTLEY[2,1], CHRISTOPH SCHNABEL[3], ANDREAS CZIFERSZKY[1], PETER FRETWELL[1], PETER CONVEY[1] and SHENG XU[4]

[1]*British Antarctic Survey, NERC, High Cross, Madingley Road, Cambridge, CB3 0ET, UK*
[2]*Department of Geography, University of Durham, South Road, Durham, DH1 3LE, UK*
[3]*NERC Cosmogenic Isotope Analysis Facility, Scottish Universities Environmental Research Centre (SUERC), Rankine Avenue, East Kilbride, G75 0QF, UK*
[4]*Scottish Universities Environmental Research Centre (SUERC), Rankine Avenue, East Kilbride, G75 0QF, UK*
daho@pcmail.nerc-bas.ac.uk

Abstract: We studied the glacial geomorphology and geochronology of two ice-free valleys in the Dufek Massif (Antarctic Specially Protected Area 119) providing new constraints on past ice sheet thickness in the Weddell Sea embayment. [10]Be and [26]Al cosmogenic surface exposure dating provided chronological control. Seven glacial stages are proposed. These include an alpine glaciation, with subsequent (mid-Miocene?) over-riding by a warm-based ice sheet. Subsequent advances are marked by a series of minor drift deposits at 760 m altitude at >1 Ma, followed by at least two later ice sheet advances that are characterized by extensive drift sheet deposition. An advance of plateau ice field outlet glaciers from the south postdated these drift sheets. The most recent advance involved the cold-based expansion of the ice sheet from the north at the Last Glacial Maximum, or earlier, which deposited a series of bouldery moraines during its retreat. This suggests at most a relatively modest expansion of the ice sheet and outlet glaciers dominated by a lateral ice expansion of just 2–3 km and maintaining a thickness similar to that of the northern ice sheet front. These observations are consistent with other reports of modest ice sheet thickening around the Weddell Sea embayment during the Last Glacial Maximum.

Introduction

Understanding the past behaviour of the Antarctic Ice Sheet and its contribution to sea level change is an important challenge for scientists and policymakers that requires models that can make reliable, robust predictions of future change. One obstacle in addressing this challenge is the lack of information on past ice sheet behaviour. Ice sheets have long but variable response times to external forcing and so, to have confidence in ice sheet models, we need to know about Antarctic ice sheet history so that its past trajectory or dynamic behaviour can be incorporated. In some cases the long-term millennial trajectory can dominate changes seen today: for example in the Ford Ranges, West Antarctica, the long-term thinning rate of *c.* 4 cm yr^{-1} over the last 10 000 yr (Stone *et al.* 2003) closely matches the satellite-altimetry measured rate of recent decades (Davis *et al.* 2005). The implication is that we have to know the millennial-scale history of the ice sheets if we are to predict their future.

For Antarctica, the greatest ice volume changes since the Last Glacial Maximum (LGM) have been in the Ross and Weddell Sea regions (Bentley 1999, Denton & Hughes 2002). Significant progress has been made in deciphering the Ross

Sea deglaciation with an emerging consensus that the area has experienced progressive thinning and grounding line retreat through the Holocene (Conway *et al.* 1999, Stone *et al.* 2003). It has also been suggested that the grounding line retreated as a 'swinging gate', hinged in the eastern Ross Sea (Conway *et al.* 1999). In contrast, the pattern and timing of deglaciation of the Weddell Sea embayment (Fig. 1) is less well known, despite accounting for as much as half of the volume change of the West Antarctic Ice Sheet (WAIS) since the LGM (Bentley 1999, Denton & Hughes 2002). This uncertainty has hampered efforts to understand the LGM volume of the ice sheet in this region, and identify if it made any significant contribution to rapid postglacial global sea level rises such as meltwater pulse 1A (Clark & Mix 2002, Bassett *et al.* 2007).

Past ice sheet thickness can be inferred from the glacial geomorphology and geochronology of trim lines, moraines, drift limits and bedrock surfaces flanking the inland mountains of Antarctica. At present the thinning history of the WAIS and East Antarctic Ice Sheet (EAIS) in the Weddell Sea embayment is primarily constrained by glacial geological data from the Ellsworth Mountains (Bentley *et al.* 2010) and the Shackleton Range (Fogwill *et al.* 2004, Hein *et al.* 2011), respectively. In the Ellsworth Mountains geomorphological
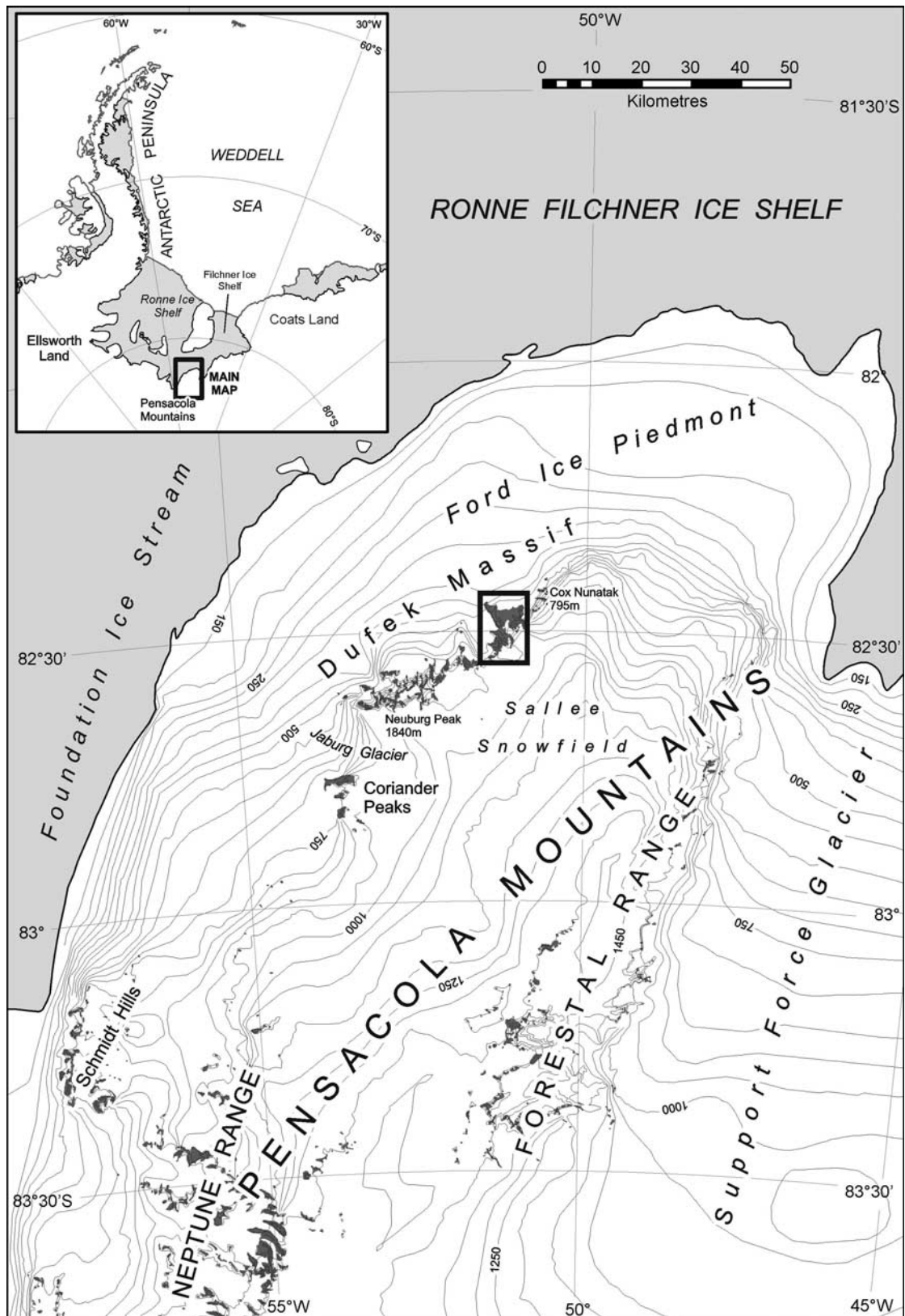
Fig. 1. Location map of the northern Pensacola Mountains showing the major mountain ranges, glaciers and other glaciological features including the Dufek Massif and Davis Valley (inset box).

analysis has shown that the original Quaternary or pre-Quaternary ice thickness change was probably 800–1000 m (Denton *et al.* 1992) and for the LGM there is geomorphological evidence for a lower trimline that takes the form of a drift limit and/or weathering break at 230–480 m above present-day ice (Bentley *et al.* 2010). In the Shackleton Range cosmogenic surface exposure dating of bedrock surfaces has shown that exposure ages between 1.16 and 3.0 Ma provide minimum estimates for the last glacial over-riding of the summit plateau (Fogwill *et al.* 2004). These ages constrained EAIS thickening to < 750 m throughout the last 3 Ma. Fogwill *et al.* (2004) also calculated erosion rates of the bedrock and obtained a range of 0.10–0.35 m Ma^{-1}. The value of 0.35 m Ma^{-1} assumes saturation and so represents the maximum erosion rate possible. Hein *et al.* (2011) showed minimal thickening in the Shackleton Range during the last glacial cycle. Collectively this work has demonstrated that LGM ice in the region was thinner than previously assumed with many of the upper slopes of the mountains remaining ice-free, implying that sea level contributions from this sector need to be revised. This supports initial analyses of an ice core drilled at Berkner Island which demonstrates that the ice rise forming the island remained a separate ice dispersal centre throughout the last glacial cycle and was not over-ridden by continental ice (Mulvaney *et al.* unpublished).

The objectives of this study were to map and survey the geomorphological features of two ice-free dry valleys in the northern Dufek Massif and to constrain past ice sheet behaviour, linking with studies in the Ellsworth Mountains to the west and Shackleton Range to the north-east. First we mapped and described the main topographic and geomorphological features, and second we carried out ^{10}Be and ^{26}Al cosmogenic surface exposure dating of glacially transported erratic rocks associated with selected geomorphological features to provide chronological constraints on the glacial history. We discuss the results with reference to published constraints on ice sheet thickness from other exposed mountain ranges around the Weddell Sea embayment.

Site description and previous work

The Dufek Massif centred at 82°24'S, 52°12'W (Fig. 1) is situated at the northern end of the Pensacola Mountains and is part of the Transantarctic Mountain range. It is approximately mid-way between the Support Force Glacier and the Foundation Ice Stream, two of the major glaciers draining northwards from the Polar Plateau into the Filchner-Ronne Ice Shelf. Approximately 60 km to the south-east is the Forrestal Range (also part of the Pensacola Mountains), which is separated from the Dufek Massif by the Sallee Snowfield, a plateau ice field that forms the southern and eastern boundary of the Dufek Massif. To the north and north-west is the Ford Ice Piedmont which

separates the Dufek Massif from the Ronne and Filchner ice shelves, *c.* 50 km to the north-west and 70 km to the north-east respectively. The nearest significant mountain chains are the Ellsworth Mountains 800 km to the west, and the Shackleton Range 400 km to the north-east.

The total area of the Dufek Massif is 11 668 km^2 and its highest point is England Peak (2150 m). Its geology has been described by Behrendt *et al.* (1974), Ford (1976, 1990) and Ford *et al.* (1978) and geophysically surveyed by Ferris *et al.* (1998). Studies of its meteorology are limited, but mean annual temperature inferred from nearby ice boreholes lies between -24.96°C, 32 km due north of the Davis Valley on the Ford Ice Piedmont in December 1957 (Aughenbaugh *et al.* 1958), and -9°C in December 1978 in the Enchanted Valley, 26 km to the south (Boyer, personal communication 2000). Near surface winds in winter are predominantly from the WNW with modelled mean winter velocities of *c.* 10 m s^{-1} (Van Lipzig *et al.* 2004). It has also been identified as an ablation area comprising two types of wind driven ablation (Van den Broeke *et al.* 2006). Type 1 includes erosion driven ablation areas, caused by 1-D and/or 2-D divergence in the katabatic wind field where solid precipitation and sublimation are small but where divergence in the snowdrift transport can be considerable. Type 2 appears to dominate within the study area and includes sublimation driven ablation areas occurring at the foot of steep topographic barriers, where temperature and wind speed are high and relative humidity low, with individual glacier valleys, serving as gates for air drainage from the plateau to the Filchner-Ronne Ice Shelf. Strongest sublimation rates occur on these localized glaciers in the Transantarctic Mountains, where widespread blue ice areas are known to exist (Van den Broeke *et al.* 2006).

The area was first visited in the International Geophysical Year (1957) and then by the USGS in 1978–79. It was on these expeditions that geologists discovered the Davis Valley and Forlidas valley (unofficial name), dry valleys, occupying 53 km^2 with 39 km^2 of this being ice-free (Behrendt *et al.* 1974). Although less than 1% of the area of the McMurdo Dry Valleys, these valleys represent the largest ice-free valley system found south of 80°S in the Weddell Sea sector of Antarctica and were reported to contain a rich geomorphological record of glacial history of the ice sheet (Boyer 1979). Some ice-free areas around the Weddell Sea embayment have scattered erratics or (rare) moraines, but in the Dufek Massif the first visitors identified that the assemblage of drift limits, moraines, abundant quartz-bearing erratics and their intersecting relationships would provide an excellent opportunity to determine constraints on the glacial history of the Weddell Sea margin. For these attributes, and its unusual biological communities (Hodgson *et al.* 2010, Fernandez-Carazo *et al.* 2011, Peeters *et al.* 2011a, 2011b) the area around Forlidas Pond and Davis Valley Ponds is designated as an Antarctic Specially Protected Area (ASPA No. 119). Boyer (1979) made geomorphological
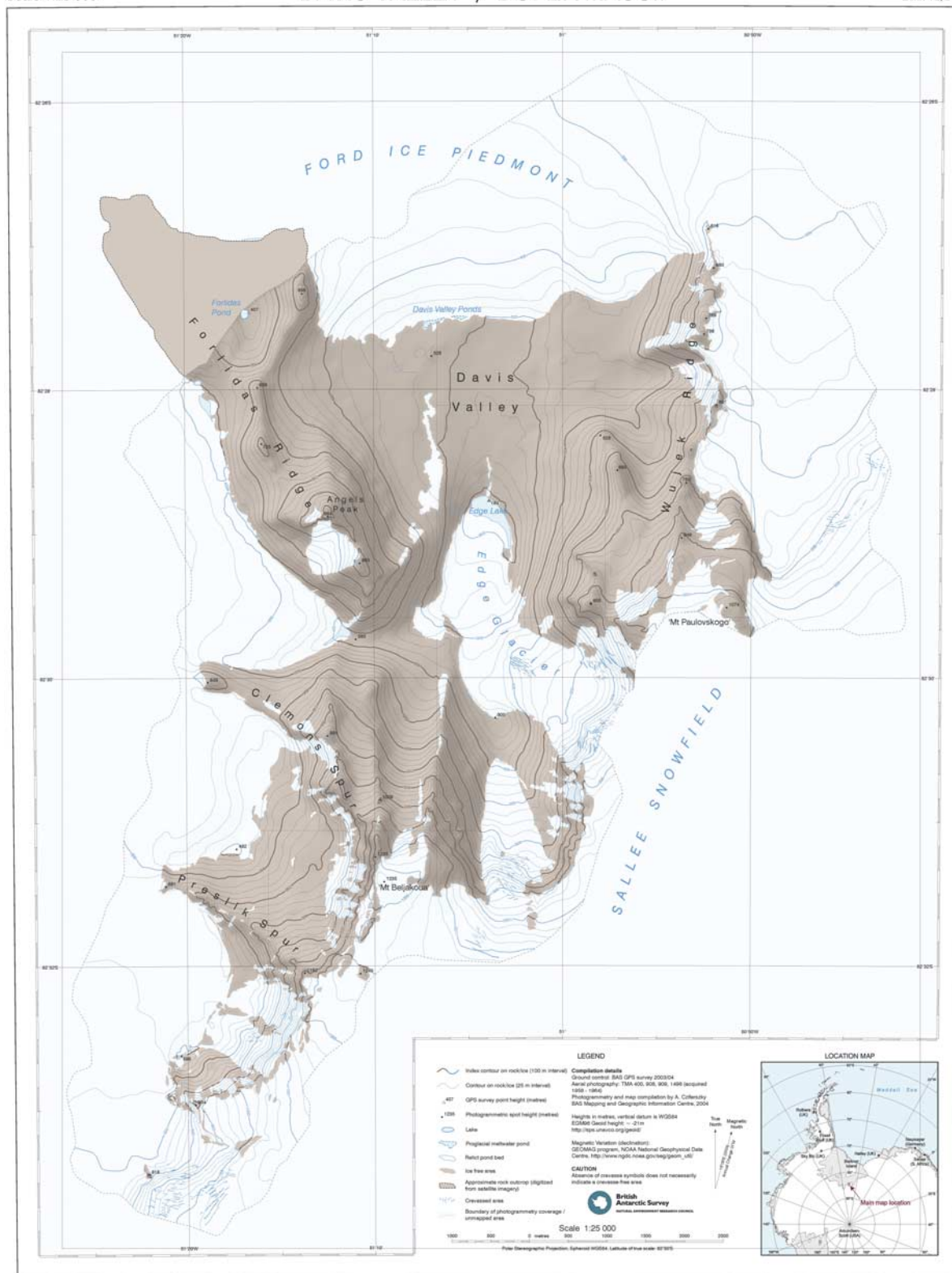
Fig. 2. Topographic map of the northern Dufek Massif and Davis Valley. A high-resolution version of this map can be downloaded from the SCAR map catalogue at http://data.aad.gov.au/aadc/mapcat/.

Fig. 3. Panorama of the Davis Valley (left) and Forlidas valley (unofficial name, right), looking south. The panorama shows the Stage 1 alpine glaciation cirques and arêtes, and Stage 2 moulded ridges, summits and breached arêtes from ice sheet over-riding. The prominent Stage 2 U-shaped breaches in the arête of Wujek Ridge can be seen on the left of the photograph. Towards the middle of the photograph small outlet glaciers can be seen descending through similar breaches into the Davis Valley, the largest of which is the *c.* 4 km long Edge Glacier.

observations not only in Davis Valley but also on Saratoga Table, a plateau nunatak located *c.* 100 km to the south of the Dufek Massif in the Forrestal Range. He was unable to provide any dates for the glacial record he described, but on the basis of geomorphological relationships he proposed the following sequence of events: 1) a very old sub-polar or temperate-type valley glaciation, 2) a former ice sheet level as much as 400 m higher than today, 3) multiple advance and retreat of local alpine ice since the last major ice advance, and 4) a complex glacial, glaciofluvial and lacustrine history. Boyer (1979) provisionally correlated the occurrence of Davis Valley erratics above 1000 m altitude with the McMurdo Sound region glacial episodes 'Taylor V-II' (Miocene to 1.6 Ma) of Denton *et al*. (1971), and the Davis Valley ice sheet deposits with the 'Taylor I' glacial episode (12 200 yr BP to present).

Methods

Geomorphological mapping and glacial geomorphology

Topographic and geomorphological maps were compiled by the Mapping and Geographical Information Centre (British Antarctic Survey) at 1:25 000 scale using aerial photographs from the United States Geological Survey (Lassiter Station 1-16 and 1-17, 1 February 1958), GPS-surveyed ground control and differential geodetic GPS survey transects were carried out using a Trimble 5700 base station and a Magellan ProMark 10CM rover unit. Altitudes were referenced to the WGS84 reference ellipsoid, and included accurate photogrammetric height measurements of key

Fig. 4. The distinctive blue ice lobes of the Ford Ice Piedmont (left) discharging into the Davis Valley.

Fig. 5. Tafoni and weathered bedrock in local gabbro and pyroxenite bedrock above the upper Stage 4 drift limit on Forlidas Ridge.
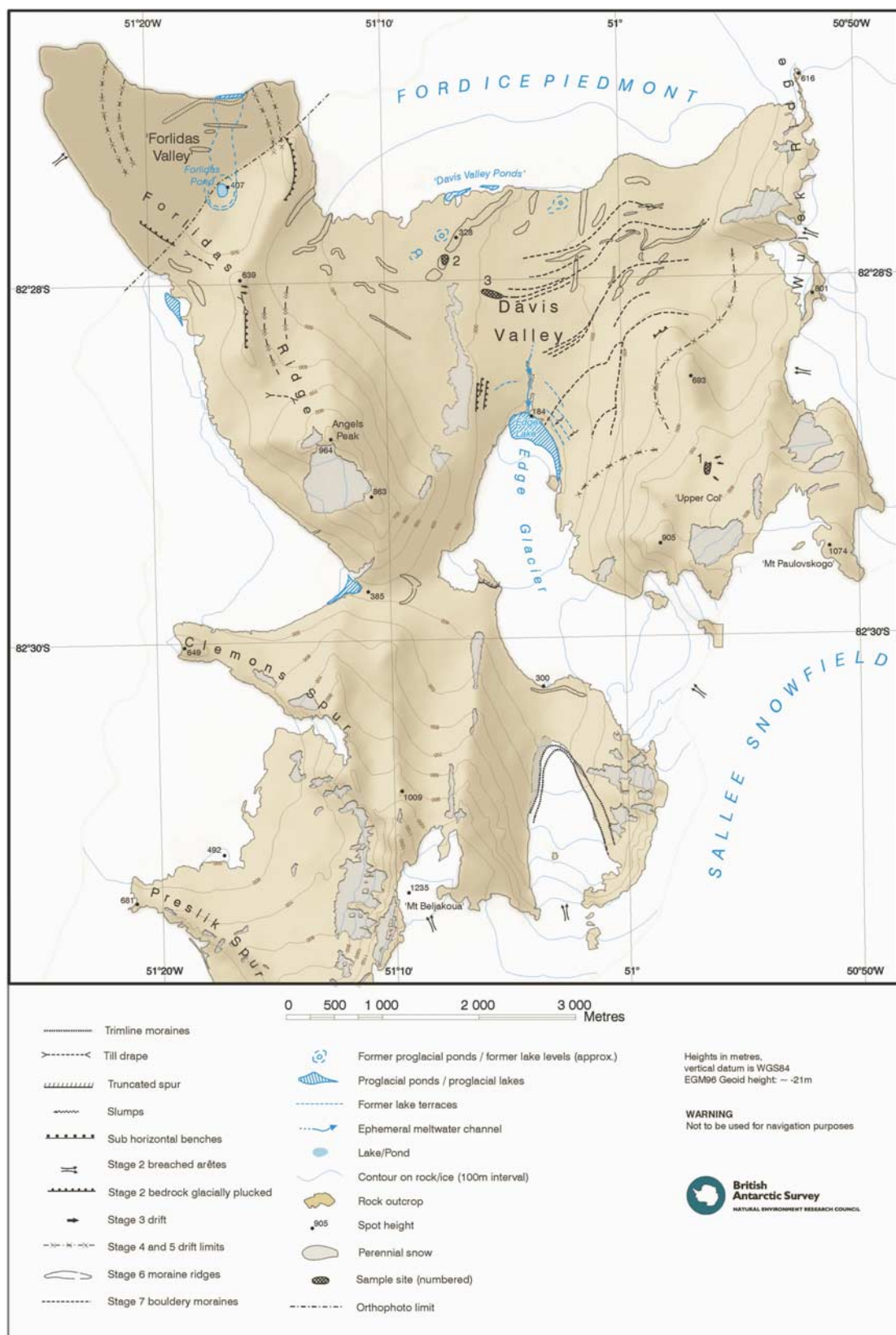
Fig. 6. Geomorphological map of the northern Dufek Massif and Davis Valley. Sampling sites for cosmogenic isotope exposure age dating are marked with cross-hatched areas labelled 1–3 on the map. A high-resolution version of this map can be downloaded from the SCAR map catalogue at http://data.aad.gov.au/aadc/mapcat/.
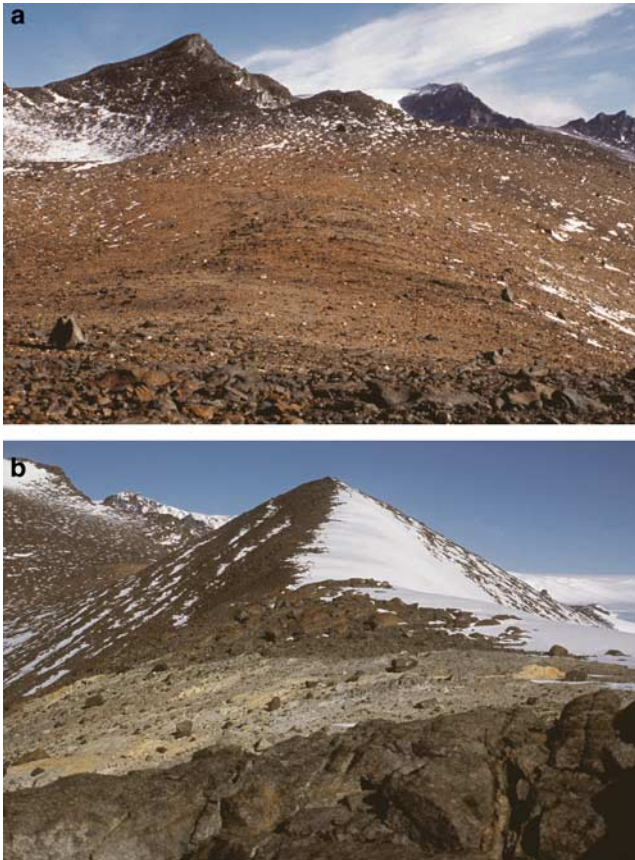
Fig. 7. a. 'Upper Col' drift from Stage 3 ice sheet advance showing Dover Sandstone erratics. **b.** Stage 3 drift on Forlidas Ridge.

Fig. 8. Stages 4 and 5 drift sheet in Davis Valley. Note the change in the diameter and relative height of the frost sorted polygons approximately mid-way across the photograph which marks the boundary between the Stage 4 and 5 drift limits. Two people are present on snow in the middle foreground for scale.

top surface of flat-topped boulders ranging from *c.* 30–80 cm in height. Each sample was marked up with orientation, edge/face details and photographed in detail and in its site context. GPS locations (including differential GPS measured altitudes) were recorded together with details of topographic shielding in 15° azimuth intervals.

Laboratory procedures, and calculations of exposure ages using the CRONUS-Earth online calculator (Balco *et al.* 2008) are outlined in the supplemental material. In the calculations the newly determined half-life of 1.389 Ma for ^{10}Be was used (Chmeleff *et al.* 2010, Korschinek *et al.* 2010).

Results

Large-scale bedrock geomorphology

The study area is located on the northern edge of the Sallee Snowfield, a 100 km long plateau ice field (Fig. 1). The Dufek Massif is part of an escarpment that descends from the Sallee Snowfield to the Ford Ice Piedmont to the north. The northern edge of the escarpment forms an alpine landscape characterized by alpine peaks, cirques and intervening arêtes (Figs 2 & 3). At its northern end are two distinctive dry valleys. In places the bedrock ridges show large-scale ice moulding including asymmetric rounded summits (roche moutonnée forms), plucked faces and prominent U-shaped breaches in the ridge - particularly Wujek Ridge to the east (Figs 2 & 3). We interpret the landscape exposed at the plateau edge as one of alpine glaciation that was subsequently completely over-ridden by an erosive (warm-based) ice sheet that formed breaches and roches moutonnées.

The Davis Valley and adjacent Forlidas valley are Antarctic 'dry valleys', with their valley floors being lower in elevation than the surrounding ice, with some over

landforms. Glacial geomorphological mapping was carried out from field observation and aerial photographs. Boyer (1979) was used as a starting point for interpretations. The main glacial features were described following the glacial land systems methods of Evans (2003).

Glacial chronology

We sampled erratics of Dover Sandstone (Ford *et al.* 1978) for ^{10}Be and ^{26}Al cosmogenic isotope dating following the protocols outlined in Gosse & Phillips (2001). Six or seven erratic samples were collected from three of the identified glacial stages. All erratics were of Dover Sandstone which differs from the local (stratiform) middle Jurassic (191–147 Ma) mafic igneous bedrock geology (Ford *et al.* 1978). Erratics showed limited rounding of the edges, limited or no spalling or pitting of boulder surfaces, and no clear evidence of previous cover by till or other sediment. This suggests that they were deposited by ice and have not been exhumed from drift sheets. Samples were taken from flat-lying areas to limit the possibility of samples having overturned or moved down-slope. Samples generally consisted of parallel-sided, 5 cm thick horizontal slabs of rock from the

Fig. 9. Drift limits in Forlidas valley showing the two distinctive Stage 4 and 5 drift limits marked by changes in polygon morphology and rock colour, and a series of less distinct limits defined by relatively minor changes in polygon morphology, in this case picked out by a light dusting of snow. Forlidas Pond can be seen in the middle of the photograph. The higher Holocene water levels have resulted in an area in the base of the valley in which large-scale frost sorted polygons are absent.

deepening, for example around Edge lake (Figs 2 & 3). For example the Davis Valley descends *c.* 160 m over 2 km between the northern ice sheet front of the Ford Ice Piedmont and Edge lake (unofficial name) and more than 1000 m from the Sallee Snowfield to the south. The northern ice sheet front is characterized by distinctive lobes of blue ice which 'flow' into the valley (Fig. 4). The shape and surface contours of the ice front are probably influenced by

Fig. 10. Stages 4 and 5 drift limits extending under Edge lake and the Edge Glacier. The transition between the sloping ice of the glacier and the sub-horizontal surface of Edge lake can be seen on the left of the image. Supraglacial debris and boulders are present both on the glacier and the lake.

Fig. 11. a. Stage 6 Davis Valley outlet glacier moraine ridges. **b.** Stage 7 bouldery moraine in the Davis Valley. **c.** Examples of the larger boulders in the bouldery moraine. The figure standing in front of the left boulder is for scale.

the morphology of the valleys directing wind patterns and hence differential ablation and sublimation. The southern part of the valley rises steeply to the escarpment edge with a number of small outlet glaciers descending from the plateau ice field through the lower saddles into the valley (Fig. 3), the largest of which is the *c.* 4 km long Edge Glacier which occupies the southern end of the Davis Valley. The valleys are therefore affected by ice both from the north and south.

Fig. 12. A boulder emerging from the blue ice margin of the Ford Ice Piedmont in the Davis Valley, illustrating the process that forms the Stage 7 bouldery moraine. A person is in the middle of the image for scale.

In Forlidas and Davis valleys bedrock surfaces and boulders above the drift sheet limits share characteristics of long-term wind erosion, including sculpting of bedrock, and tafoni more than a metre in diameter (Fig. 5) but give way to glacial erosion features in the valleys below the drift limit. At the time of visiting there was limited windblown debris on the lake ice surfaces, local snow patches, or the neighbouring glacial surfaces.

Depositional features

Within the valleys there is an extensive glacial geomorphological record of multiple glacial advances and

Fig. 13. Forlidas Pond. The higher water level of the much larger proglacial lake from which the pond originated is 17.7 m above the present water level and is delineated by salt efflorescence on the rocks and the absence of well-formed frost sorted polygons. A series of lake terraces that can be seen immediately around the pond marks a series of lower lake levels formed in the mid-Holocene before the present water level was reached.

Fig. 14. Palaeoshorelines above the current shoreline of Edge lake looking from west to east. These are overlain by the most distal of the Stage 7 bouldery moraines, and bisected by a meltwater gully across the middle of the image. The 'Upper Col' sampling site and Stage 3 drift are visible at the top of the image, with the main arête behind.

retreats (Boyer 1979). Features include overlapping valley glacier moraines, ice sheet moraines, lake shorelines, ice eroded surfaces, well developed patterned ground and glacial erratics (Fig. 6).

In at least two high areas of the valleys there is depositional evidence of glacier advance to limits over 600 m altitude. The first of these is at 'Upper Col' (Fig. 6,

Table I. Cosmogenic isotope sample data. All samples are erratics of Dover Sandstone.

Sample name	Latitude (°S)	Longitude (°W)	Elevation (m)	Sample thickness (cm)	Sample density (g cm^{-3})	Shielding factor
DVAM1	82.4664	51.1225	353	4.19	2.49	0.998
DVAM2	82.4651	51.1246	349	4.70	2.82	0.998
DVAM3	82.4664	51.1280	340	3.43	2.55	0.998
DVAM4	82.4651	51.1275	343	3.46	2.62	0.998
DVAM5	82.4651	51.1289	345	3.72	2.60	0.998
DVAM6	82.4651	51.1303	345	4.29	2.57	0.998
DVRM1	82.4684	51.0823	302	3.41	2.67	0.997
DVRM2	82.4684	51.0823	302	3.46	2.60	0.997
DVRM3	82.4685	51.0754	300	4.58	2.67	0.990
DVRM4	82.4682	51.0658	294	4.53	2.68	0.997
DVRM5	82.4849	51.0583	294	3.92	2.46	0.997
DVRM6	82.4681	51.0608	296	2.62	2.55	0.997
DVRM7	82.4681	51.0608	296	3.23	2.66	0.997
DVUC1	82.4829	50.9414	755	2.04	2.38	0.993
DVUC2	82.4830	50.9413	760	5.32	2.66	0.993
DVUC3_1	82.4830	50.9402	760	3.05	3.13	0.992
DVUC3_2	82.4830	50.9402	760	3.05	3.13	0.992
DVUC4A	82.4829	50.9401	761	4.45	2.33	0.992
DVUC4B	82.4829	50.9401	761	4.45	2.33	0.992
DVUC4JUN	82.4829	50.9401	761	4.45	2.58	0.992
DVUC5	82.4829	50.9399	760	1.86	2.45	0.993
DVUC6	82.4828	50.9340	759	5.51	2.60	0.993
DVUC7	82.4830	50.9424	749	4.42	2.38	0.993

Table II. Cosmogenic isotope data.

Sample name	^{10}Be AMS ID SUERC	^{10}Be concentration[1] (10^6 at g^{-1} qtz)	Production rate ^{10}Be spallation[2] (at g^{-1} yr^{-1})	Production rate ^{10}Be muons[2] (at g^{-1} yr^{-1})	^{10}Be exposure age[3] (kyr)	Total uncertainty ^{10}Be exposure age[4] (kyr)	^{26}Al AMS ID SUERC	^{26}Al concentration[5-7] (10^6 at g^{-1} qtz)	^{26}Al/^{10}Be[8-9] (at/at)
DVAM1	b396	5.35 ± 0.22	7.79	0.221	813 ± 42	97	n.a.	n.d.	n.d.
DVAM2	b397	3.35 ± 0.12	7.69	0.22	476 ± 20	51	a237	13.67 ± 0.70	4.08 ± 0.26
DVAM3	b499	5.99 ± 0.24	7.73	0.22	945 ± 48	115	n.a.	n.d.	n.d.
DVAM4	b291	5.22 ± 0.18	7.74	0.22	794 ± 34	91	a103	15.77 ± 0.86	3.02 ± 0.20
DVAM5	b500	6.46 ± 0.25	7.74	0.22	1039 ± 53	130	n.a.	n.d.	n.d.
DVAM6	b292	2.72 ± 0.10	7.71	0.22	376 ± 15	39	a101	9.91 ± 0.45	3.64 ± 0.21
DVRM1	b286	1.59 ± 0.06	7.43	0.217	219 ± 8	22	a98	6.70 ± 0.35	4.23 ± 0.27
DVRM2	b501	3.24 ± 0.13	7.43	0.217	476 ± 21	51	a247	11.16 ± 0.59	3.45 ± 0.23
DVRM3	b280	5.02 ± 0.17	7.29	0.216	814 ± 34	94	a92	21.45 ± 1.37	4.27 ± 0.31
DVRM4	b287	4.48 ± 0.16	7.30	0.216	707 ± 30	79	n.a.	n.d.	n.d.
DVRM5	b497	5.26 ± 0.21	7.35	0.216	853 ± 42	102	n.a.	n.d.	n.d.
DVRM6	b290	5.91 ± 0.21	7.44	0.216	975 ± 44	118	a105	17.08 ± 0.76	2.89 ± 0.16
DVRM7	b399	5.23 ± 0.19	7.39	0.216	842 ± 38	99	a238	20.74 ± 1.01	3.96 ± 0.24
DVUC1	b282	9.99 ± 0.36	11.53	0.256	1103 ± 52	138	a104	47.26 ± 2.14	4.73 ± 0.27
DVUC2	b400	8.50 ± 0.31	11.25	0.255	921 ± 42	110	a239	43.13 ± 2.07	5.08 ± 0.31
DVUC3_1	b238	7.01 ± 0.24	11.4	0.256	715 ± 30	80	a84	9.91 ± 0.49	1.41 ± 0.09
DVUC3_2	b239	7.10 ± 0.26	11.4	0.256	727 ± 32	82	n.a.	n.d.	n.d.
DVUC4A	b236	13.80 ± 0.48	11.38	0.256	1798 ± 102	273	n.a.	n.d.	n.d.
DVUC4B	b237	14.62 ± 0.50	11.38	0.256	1896 ± 111	296	n.a.	n.d.	n.d.
DVUC4JUN	b281	14.63 ± 0.52	11.34	0.255	1992 ± 121	320	a95	55.79 ± 3.05	3.81 ± 0.25
DVUC5	b285	6.90 ± 0.25	11.59	0.257	688 ± 29	77	a99	28.32 ± 1.26	4.10 ± 0.23
DVUC6	b401	10.82 ± 0.39	11.24	0.255	1273 ± 64	168	n.a.	n.d.	n.d.
DVUC7	b498	12.58 ± 0.49	11.27	0.254	1579 ± 94	229	n.a.	n.d.	n.d.

at = atom, n.d. = not determined.

[1] Based on normalization according to Nishiizumi *et al.* (2007): 2.79 * 10^{-11} as ^{10}Be/^{9}Be for NIST SRM4325.

[2] One sigma uncertainty including 2.5% for uncertainty of Be concentration of carrier solution.

[3] CRONUS-Earth calculator (Balco *et al.* 2008), wrapper script 2.2, main calculator 2.1, constants 2.2.1, muons 1.1, production rates related to ^{10}Be half-life of 1.39 Myr and Antarctic air pressure.

[4] CRONUS-Earth calculator, wrapper script 2.2, main calculator 2.1, constants 2.2.1, muons 1.1; related to a ^{10}Be half-life of 1.39 Myr; constant production rate scheme Lal/Stone.

[5] One sigma analytical uncertainty (does not include uncertainty of production rate).

[6] Based on normalization to Purdue standard material Z92-0222 with a nominal 26Al/27Al ratio of 4.11 * 10^{-11} - in agreement with Nishiizumi's standards (Nishiizumi 2004).

[7] One sigma uncertainty including the uncertainty of the determination of Al in quartz.

[8] Related to an initial production rate ratio of 6.75.

[9] One sigma uncertainty.

informal name), at 760 m, and consists of a yellowish brown drift deposit occupying the edge of a shallow depression to the west of the Wujek Ridge (Fig. 7a). The drift has a well-defined upper limit and is characterized by distinctive colour and lithological composition, containing abundant erratics of yellow Dover Sandstone. Outside and above this drift, the surface debris cover is composed exclusively of the local gabbro and pyroxenite bedrock (Ford *et al.* 1978). The second site is on Forlidas Ridge (Fig. 6, marked as Stage 3 drift; Fig. 7b) just south of the bedrock summit at 639 m. It consists of a pale creamy band of regolith, probably derived from weathering of a pegmatite or aplite dyke (Ford *et al.* 1978) that cuts across the ridge, over which are scattered numerous erratic clasts of local bedrock and occasionally of Dover Sandstone. Both deposits sit on areas of relatively level terrain away from steep slopes and so the surface cover was more probably transported by ice rather than rock fall. Field

observations from a distance suggest that there may be equivalent units in the unvisited high southern parts of the valleys around Clemons Spur and Presilik spur (unofficial name). The Upper Col drift deposit records a glacier advance that spilled down from Wujek Ridge to 760 m altitude whilst the drift deposit on Forlidas Ridge records a glacier advance spilling over the ridge from the west.

Below these sites the valleys are occupied by two distinctive drift sheets marked by the presence of frost sorted polygons consisting primarily of large clasts and boulders (Fig. 8). The larger polygons are typically > 35 m diameter, *c.* 2 m high and grade into sorted stripes as slopes increase and the networks become more elongate down-slope (cf. Kessler & Werner 2003). The upper extent of the upper drift (altitude < *c.* 600 m) is dark reddish brown, distinct, abrupt and can be traced along the margins of both Davis and Forlidas valleys. A second lower drift limit (altitude *c.* 550 m) can

be distinguished on the basis of a minor change in the degree of weathering, and a marked increase in the diameter and height of the polygons (Figs 8 & 9). This limit cannot be traced as extensively as the upper drift, but where they are both present their upper limits are sub-parallel. A further series of less distinctive drift limits marked by subtle changes in polygon morphology (diameter, height, weathering) are also evident. The drift sheets extend under the present-day ice sheet margin, and also under the Edge Glacier (Fig. 10).

The floor of Davis Valley contains a complex set of intersecting moraine ridges. The largest of these are large moraine ridges, 50–200 m wide and 15–20 m high extending for more than 1 km just south of the Davis Valley ponds (Fig. 3, Stage 6; Fig. 11a). The moraines are symmetrical with rounded crests and composed of relatively well sorted cobble to small boulder surface material. The ridges do not show advanced development of frost sorted polygons, although there are occasional cracks (ice wedges?) on the ridge flanks. In the central part of the Davis Valley close to the present-day ice sheet margin we mapped some of the more prominent of these moraines including an arcuate western ridge and a linear eastern ridge. Both these ridges extend under the ice sheet (Fig. 6). There is a complex of smaller ridges with similar morphology in two areas located outside of these larger ridges towards the sides of the valley. These are less continuous and orientated obliquely to the ice sheet margin. On the western side of the valley some of these moraines also extend under the ice sheet margin (Fig. 6). Minor moraine ridges also occur in similar orientations in the northern part of Forlidas valley but unlike Davis Valley these are overprinted by the drift sheet polygons. Small moraine ridges with similar morphology occur at 82°29'40"S, 051°09'00"W, just north of Clemons Spur, between the eastern margin of the ice sheet and the Edge Glacier, and at 82°28'S, 051°19'W, along the west flank of Forlidas Ridge, close to the eastern margin of the ice sheet.

Superimposed over the floor of the Davis Valley are a series of distinctive bouldery moraines (Fig. 11b). The moraines can be traced for over 2 km in some parts of the valley and are made up predominantly of large boulders of the local bedrock (Fig. 11c), together with a much smaller component of Dover Sandstone blocks. The proportion of the dark local rock in these bouldery moraines is much larger than that of the drift sheets and moraine ridges over which they are draped, and so from a distance they stand out as dark grey linear features. The individual moraines are concentric and sub-parallel to the present-day margin of the Ford Ice Piedmont, including the two distinctive blue ice lobes that penetrate into Davis Valley (Fig. 4). Deposition of boulders of the same lithology can be seen at the present-day ice front (Fig. 12). These moraines are confined to the eastern side of Davis Valley and extend to just over 400 m altitude. They are not present in Forlidas valley. To the south the small outlet glaciers have small

moraine loops parallel to their current margins, consistent with deposition at expanded positions.

Lacustrine and glaciofluvial features

Both valleys contain frozen water bodies. In Forlidas valley, Forlidas Pond (51°16'48"W, 82°27'28"S) is a perennially frozen, shallow pond 1.63 m deep and 90.3 m in diameter (Figs 9 & 13). Forlidas Pond is an isolated remnant of a formerly much more extensive proglacial lake. This lake formerly had water levels up to 17.7 m above present - delineated by salt efflorescence on the rocks and a series of lake terraces at 11.6 m, 8.61 m, 4.16 m and 1.25 m above the present lake level (Hodgson, unpublished data). Evaporation of this once larger water body has resulted in the accumulation of a hypersaline slush (c. 4 x greater than the salinity of seawater), underlying the ice at the bottom of the pond. An ephemeral proglacial meltwater pond also occurs where the valley meets the Ford Ice Piedmont, and two further ponds are present west of Forlidas Ridge. A series of small extant proglacial meltwater ponds, the Davis Valley Ponds, similarly occurs along the blue ice margin of the northern Davis Valley at 51°05.5'W, 82°27.5'S and 51°07'W, 82°27.55'S (Figs 3 & 4) whilst south of this a number of remnant pond beds mark the position of former proglacial ponds, probably formed during periods of ice advance into the valley (Hodgson et al. 2010). Edge lake, a perennially frozen pro-glacial lake at the terminus of the Edge Glacier is surrounded by a series of four or five depositional proglacial lake ice-push shorelines cut into the valley side, particularly near the eastern terminus of the glacier (Fig. 14). On the western side a series of sub-horizontal benches in bedrock may mark former limits of the
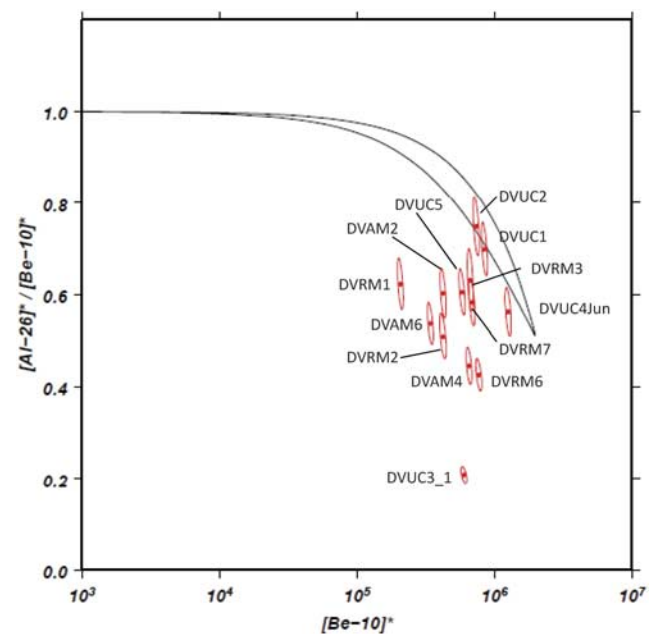

Fig. 15. ^{10}Be-^{26}Al co-isotopic diagram.

Table III. Maximum erosion rate for Upper Col samples. Calculated with the CRONUS online calculator (Balco *et al*. 2008) with data from Table I and Table II.

Sample name	Erosion rate (m Myr^{-1})	Internal uncertainty (m Myr^{-1})	External uncertainty (m Myr^{-1})
DVUC1	0.47	0.03	0.08
DVUC2	0.54	0.03	0.08

Edge Glacier. The surface of the lake ice on Edge lake has an uneven domed surface topography suggesting that it has accumulated from successive surface meltwater refreezing events, and has experienced enhanced ablation near the edges. Seasonal meltwater was observed on the eastern margin of the glacier during the sampling campaign. Supraglacial debris in the form of boulders and cobbles is present both on the Edge Glacier and Edge lake (Fig. 14).

Incised dry stream channels and water erosion features are evident within Davis Valley (Fig. 6). Some appear to have been recently active, fed by glacial meltwater but most do not appear to be related to present-day snow or ice masses and so are probably relict features. The presence of liquid water at or near the surface of all the water bodies, and even small glacial melt streams on the Edge Glacier, illustrates the ability of the relatively large areas of bare rock and soil to absorb solar radiation and emit heat causing local ice and snow melt.

Glacial chronology: cosmogenic isotope exposure ages

In order to provide a chronology for the glacial history we sampled some of the landforms described above for cosmogenic isotope analyses. We concentrated on clearly defined landform limits without disturbance by polygonisation and periglacial activity, and in order to encompass the greatest possible age range of the glacial history. We were also constrained in the current study to [10]Be and [26]Al analysis and so have focussed solely on those quartz-bearing lithologies, especially the Dover Sandstone erratics found throughout the

valley. Sites included the following three areas (see numbered cross hatched areas in Fig. 6 for locations):

1) Erratics lying on bedrock on the Upper Col at *c.* 700 m altitude (the lowest point in the Davis Valley is 184 m altitude) were used to constrain the age of the drift that was deposited in Upper Col and marks the last major over-riding of the ridges surrounding Davis Valley (cross hatched area labelled 1 on Fig. 6; Fig. 7a). This was the oldest event that could likely be dated using [10]Be since earlier events were erosional and affected the gabbro bedrock.

2) Erratics lying on the largest outlet glacier moraine ridges in northern Davis Valley (cross hatched area labelled 2 on Fig. 6; Fig. 11a), recording expansion of the Edge Glacier and other outlet glaciers discharging into the Davis Valley. Although the geomorphology shows that these moraines were over-ridden by the final ice sheet advance, our interpretation was that if the ice sheet advance was short-lived (and non-erosive?) with limited burial then we might be able to obtain a reasonable estimate of the outlet glacier moraine age.

3) Erratics deposited in bouldery moraines in the Davis Valley that mark the most recent retreat of the Ford Ice Piedmont (cross hatched area labelled 3 on Fig. 6; Fig. 11b). We selected the most prominent of a series of these bouldery moraines deposited across the valley floor sub-parallel with the current ice sheet margin. The aim of sampling these moraines was to provide age constraints on the most recent ice sheet retreat.

Sample data are in Table I and cosmogenic isotope data are shown in Table II. In order to understand periods of exposure and re-burial during sample history we analysed [26]Al-[10]Be pairs for most samples, and used a two-isotope plot (Fig. 15) (Bierman *et al*. 1999). The location of individual samples on this plot can indicate (but not mandate) whether they have had continuous exposure histories (those samples that plot within the erosion island). Samples that plot below the erosion island have complex exposure histories, with at least one period of burial. We discuss below the samples on

Table IV. Glacial stages inferred from geomorphological evidence in the Davis Valley.

Glacial stage	Description	Geomorphological evidence	Age constraint (*inferred)
1	Alpine glaciation	Cirques and arêtes that incise the escarpment edge	Early Miocene
2	Ice sheet over-riding (warm-based)	Moulding and plucking of several ridges and summits and breaching of some pre-existing arêtes	14.2–13.8 Ma*
3	Outlet glacier and ice sheet advance	Drift from outlet glaciers breaching Wujek Ridge and Forlidas Ridge	> 1.0–1.8 Ma
4	Ice sheet advance to upper drift limit in valley	Drift sheets in the valleys and drift limits along the bounding ridges	> 1 Ma*
5	Ice sheet advance to lower drift limit in valley	A lower drift limit along the bounding ridges	MIS5–>1 Ma*
6	Advance and retreat of outlet glaciers	Moraine ridges in the centre of Davis Valley	Interglacial MIS5 or earlier*
7	Advance and retreat of the Ford Ice Piedmont	Bouldery moraines in Davis Valley	LGM or earlier*

each of the three landforms that we attempted to date. In each case the ages we discuss are minimum ages because they assume zero erosion: accounting for the (unknown) amount of erosion would increase the ages.

Davis Valley Upper Col erratics (DVUC)

We sampled seven erratics from Upper Col. The two least weathered samples plot within the erosion island, namely DVUC1 (^{10}Be age = 1.1 Ma, altitude = 755 m) and DVUC2 (0.9 Ma, altitude = 760 m). One other sample plots close to the erosion island, namely DVUC4JUN (1.99 Ma, altitude = 761 m). Two other Upper Col samples for which there are both Al and Be data do not plot in the erosion island (DVUC5 (0.7 Ma, altitude = 760 m) and DVUC3_1 (0.7 Ma, altitude = 760 m)), and indeed the latter sample sits the furthest away from the erosion island of any sample in Davis Valley. However, there are several DVUC samples that do not have Al data but have ^{10}Be ages consistent with the oldest of the samples lying within the erosion island (Table II, Fig. 15). Replicates on sample DVUC4 (altitude = 761 m) show it has a minimum exposure age of 1.8–1.9 Ma, whilst DVUC6 (altitude = 759 m) and DVUC7 (altitude = 749 m) yield minimum ages of 1.3 and 1.6 Ma, respectively. Given these consistently old ages, and the fact that a majority of DVUC samples with combined Be-Al data have isotopic ratios that are consistent with continuous exposure then we suggest that the Upper Col has been exposed for well over 1 Ma since the advance to this location (to 750 m altitude or higher), and perhaps for as much as 2.0 Ma.

It is also possible to take this one step further and calculate maximum long-term erosion rates for those samples within the erosion island. This requires the assumption that the samples have reached secular equilibrium. These yield rates of 0.47–0.54 m Myr^{-1} (Table III).

Davis Valley outlet glacier moraine ridges (DVAM)

We sampled six erratics on a prominent moraine ridge that was deposited by a formerly expanded Edge Glacier flowing north. The two-isotope plot shows that all three of the samples for which we have paired Be-Al analyses have complex exposure histories with at least one period of burial (Fig. 15). Those samples with Be-Al paired analyses show consistently younger Al ages than Be, implying burial and probable reworking and that these ages cannot be used to infer the precise timing of glacier advances. Even the youngest of these paired ages is highly discordant. It is also clear from the ^{10}Be ages alone that there is a large spread of ages (376–1039 ka), which can be an indicator of a (partly) reworked deposit.

Davis Valley Ford Ice Piedmont bouldery moraines (DVRM)

Five of the seven samples from the bouldery moraines associated with advance and retreat of the Ford Ice Piedmont margin have paired Be-Al analyses and all of these show complex exposure histories. Ages range between 219 and 975 ka, but they show consistently younger Al ages than Be ages, and even the youngest sample (DVRM1) shows a discordant age pair, implying that it cannot be used to estimate the age of this deposit. We suspect that the high recycling ratio is probably due to our selection of quartz-bearing lithologies (Dover Sandstone) for analysis. The moraines are dominantly composed of igneous clasts, and indeed that is the lithology we have observed emerging at the present-day margin (Fig. 12).

Discussion

We have mapped the glacial geomorphology of two dry valleys in the northern Dufek Massif, building on the work of Boyer (1979). We interpret the intersecting relationships between bedrock landforms, drift limits, and moraines as the result of seven stages of glaciation (Table IV). The evidence for these is described below:

Glacial stages
Stage 1: Alpine glaciation
The alpine glaciation that formed the cirques and arêtes that incise the escarpment edge is the earliest part of the glacial history that can be identified. At this time the plateau was probably occupied by a small ice field - the precursor to the Sallee Snowfield. The age of this alpine glaciation is unknown.

Stage 2: Ice sheet over-riding
The moulding and plucking of several ridges and summits, and breaching of some pre-existing arêtes suggest that following the alpine glaciation the area was over-ridden by a warm-based ice sheet. This ice flow was directed to the north. The strongly weathered higher surfaces (tafoni, ventifacts, honeycombing, etc) formed after ice retreat are similar to those found in the Shackleton Range on the higher summits. It may be that this over-riding glaciation dates to a major expansion of the Antarctic Ice Sheet which elsewhere has been dated at the middle Miocene climate transition (MMCT), 14.2–13.8 million years ago (Shevenell *et al.* 2004), and the rapid cooling at 13.9 million years ago in the McMurdo Dry Valleys (Lewis *et al.* 2008).

Stage 3: Outlet glacier and ice sheet advance
At some time after the warm-based ice sheet had retreated there was a minor re-advance when an outlet glacier breached the Wujek Ridge to occupy the Upper Col at 760 m, 576 m higher than the lowest part of the Davis Valley, and the ice sheet margin spilled over Forlidas eastern ridge just south of the peak at 639 m. If these drift limits are related then it suggests ice thickening and expansion occurred from the south and the west, involving both the Sallee Snowfield and the Ford Ice Piedmont.

Equivalent advances may have occurred elsewhere in the high southern parts of the valleys but were not surveyed. The cosmogenic isotope data suggests that this advance to the Upper Col occurred > 1.0 Ma (Table IV).

Stage 4: Ice sheet advance to upper drift limit in valley
The drift sheets in the valleys and drift limits along the bounding ridges shows that the valleys were occupied by ice from an expanded ice sheet margin and extended outlet glaciers breaching the southern escarpment. The upper drift limit demonstrates that these ice masses merged depositing a thick drift sheet which may not have reached the heights of the earlier advances of the Sallee Snowfield over Wujek Ridge and across the Upper Col sampling site, or the advance of the ice sheet over Forlidas Ridge. After retreat, periglacial activity initiated the development of frost sorted polygons across the surface of the drift sheet. This drift includes evidence of rocks that have been disintegrated to clay and rock particles forming soils which elsewhere in Antarctica occur in areas that have been exposed for more than a million years (Fogwill *et al.* 2004).

Stage 5: Ice sheet advance to lower drift limit in valley
A second advance or still stand to closely parallel limits deposited the lower drift sheet. The colour difference and different frost polygon 'texture' suggests a significantly different weathering history (age) to the upper drift. On retreat periglacial activity again initiated the development of a new set of frost sorted polygons. A number of less distinctive and discontinuous drift limits marks possible still stands during this retreat. The apparent extension of the polygonised drift sheets under the margins of the present-day ice sheet and the margins of the Edge Glacier implies that between these two advances, and after the second, the Ford Ice Piedmont and Edge Glacier retreated to less extensive positions than the present-day.

Stage 6: Advance and retreat of outlet glaciers
The large moraine ridges in the centre of Davis Valley are not polygonised and so we interpret them as postdating the Stage 5 drift sheet. The orientation of the moraine ridges and the absence of well developed frost sorted polygons in the central Davis Valley are consistent with an expanded Edge Glacier combined with the other outlet glaciers from the Sallee Snowfield that flowed north to meet and merge with the Ford Ice Piedmont. The outermost (westernmost and easternmost) ridges record the former margin where the Edge Glacier merged with the ice sheet piedmont and thus spread laterally. The central ridges record a former limit of the expanded Edge Glacier. The fact that these ridges extend under the ice sheet margin shows that Edge Glacier expanded when the Ford Ice Piedmont was less extensive than it is now. The minor moraine ridges in Forlidas valley, immediately west of Forlidas Ridge, and north of Clemons Spur are interpreted as marking a formerly more expanded ice sheet margin. There is a strong association between the location of ice-marginal melt ponds and these moraines: we discuss this in more detail below. The outer oblique moraines record the merging of the Edge Glacier and the ice sheet margin of the Ford Ice Piedmont, and the inner moraines record the subsequent retreat front of the Edge Glacier. The final retreat of the Edge Glacier probably resulted in the deposition of the lake shorelines and possibly the sub-horizontal benches around Edge lake. To the west of the Edge Glacier a similar expansion of the ice sheet extended the western lobe into the valley below Clemons Spur. A looping recessional moraine marks the limit of this advance.

The cosmogenic isotope data cannot be used to infer minimum ages for this advance and retreat of the outlet glaciers because the erratics have most probably been transported between different locations on the valley floor and so the most recent time of exposure cannot be calculated. In theory it is possible to estimate minimum total exposure history (i.e. exposure time plus minimum burial time) for each erratic. However, this requires two assumptions: i) that erratics have not been exposed at substantially higher elevations in their history, and ii) that larger (> 10 cm thick) erratics have not been turned over during their complex history. Given that the nearest outcrops of Dover Sandstone are tens of kilometres away and at 1000 m altitude the first assumption is difficult to sustain. Similarly, it seems unlikely that individual erratics would not be turned or rolled by over-riding ice during reworking.

Stage 7: Advance and retreat of the Ford Ice Piedmont
The most recent stage has been the advance and retreat of the Ford Ice Piedmont ice sheet margin into the northern part of Davis Valley. This is particularly well-recorded by the bouldery moraines in the eastern half of the valley. The lack of bouldery moraines in the western half of the Davis Valley and in Forlidas valley probably relates to differences in supraglacial debris supply, which may be derived from the west side of Wujek Ridge. We interpret these moraines as marking an expanded ice margin extending at least 2.5 km down valley to (and presumably under) the current location of the Edge Glacier terminus at proglacial Edge lake, which then retreated with a series of at least seven to ten still stands. The most distal of these boulder moraines overlies the Edge lake shorelines described above (Fig. 14). The present-day ice front of the Ford Ice Piedmont is a blue ice margin where boulders are being transported to the face of the ice and subsequently fall off (Fig. 12). The bouldery moraines would have formed during periods of equilibrium between the advance of the glacier and continued ablation and melting of the ice front. There is no concentration of boulders along the present-day ice front suggesting it is not currently in an equilibrium position. Radiocarbon dating of the former shorelines of Forlidas Pond shows that the ice sheet had retreated from Forlidas and Davis

valleys prior to the mid-Holocene (Hodgson, unpublished data). This suggests that the bouldery moraines record the maximum advance position of the Ford Ice Piedmont at the LGM and its subsequent retreat, although with no LGM age constraint, we cannot rule out their formation during an earlier glaciation. The outlet glaciers to the south are also currently in retreat as evidenced by abandoned looping recessional or trimline moraines.

The results of cosmogenic isotope analyses of the Dover Sandstones within these bouldery moraines suggests that they may all be reworked from earlier glacial advances into the valley from the south, rather than deposited directly from the ice margin to the north. The range of exposure ages suggest that these Dover Sandstone erratics may have been moving around the valley between ice sheet and glacier margin for upwards of 1 Ma. We can, however, provide minimum age constraints on these moraines by using the evidence for formerly more extensive water bodies over the drift surface. For example, radiocarbon dating of the former water levels of Forlidas Pond shows that the highest water levels occurred in the mid-Holocene before 2625 calendar yr BP, postdating the final retreat and formation of the ice sheet moraines (Hodgson et al., unpublished data).

In summary, our data show that the erratics in the floor of the Davis Valley have had a complex exposure history and may well be reworked in turn by alternating outlet glacier and ice sheet advances. The cosmogenic isotope analysis can demonstrate that the advance to the Upper Col occurred at > 1 Ma (Table IV), but that the ages of the outlet glacier and ice sheet advances remain unclear because of a high recycling ratio. We suggest that, for the case of the ice sheet moraines at least, this is because the Dover Sandstone erratics are probably not derived from the ice sheet margin itself, but instead are reworked from earlier deposits. We also suggest that only the most extensive over-riding advances, with substantial flow out of the valley will be capable of transporting significant quantities of material away from the valley.

Basal regime of the ice sheet and the role of marginal water ponding

The glacial history above, based on observations of striations and erosional features, shows that there have been both dry-based and wet-based glacial episodes. Erosional landforms suggest that early glacial episodes (Stages 1 and 2) were wet-based, whist the later phases (Stages 3–5 and 7) are all consistent with a dry-based ice sheet. In this context the landforms associated with Stage 6 are puzzling. The large constructional moraine ridges with relatively little bouldery material are more characteristic of a temperate glacial margin. We have mapped a strong association between marginal melt ponds and the Stage 6 moraine ridges in the dry valleys. One possible explanation is that, like today, both ice fronts were characterized by the occasional presence of meltwater and melt ponds. If there was substantial water around the margin

then this could have promoted subglacial erosion and deformation of pre-existing sediment at the margin of the ice, and/or mobilization and deposition by meltwater, and thus enable deposition of these large ridges. The unusual orientations may have resulted from the interaction of the two respective ice fronts of the Ford Ice Piedmont and the Edge Glacier. Some evidence for this role of water in moraine deposition is the close association of moraines and ice marginal ponds west of Forlidas Ridge and north of Clemons Spur and northern Forlidas valley (Fig. 6). Moraines are not found anywhere else along this margin.

Regional comparisons

The closest sites in the region for which the glacial history has been studied are the Shackleton Range (Kerr & Hermichen 1999) and Ellsworth Mountains (Denton et al. 1992, Bentley et al. 2010). At each of these sites there is evidence of an alpine glaciated landscape that has been over-ridden (Shackleton Range - as evidenced by the more rounded nature of the mountains, more limited development of cryoturbation features, and general uniformity of the terrestrial habitat) or partly submerged (Ellsworth Mountains) by a thicker warm-based ice sheet. In the Shackleton Range the warm-based over-riding is interpreted to date from at least 1–3 Ma (Fogwill et al. 2004). Our data from the erratics in the Upper Col of Davis Valley are consistent with these results as they give a minimum age for the drift in the col of > 1.0 Ma. This drift postdates the over-riding warm-based glaciation, and so this date is also a minimum estimate of the timing of the shift in basal ice sheet regime from warm- to cold-based.

The calculated maximum erosion rates for Davis Valley (0.47–$0.54 \, m \, Ma^{-1}$) are slightly higher than those for the Shackleton Range (0.1–$0.35 \, m \, Ma^{-1}$) (Fogwill et al. 2004) but might be accounted for by lithological contrasts - the Dover Sandstone we sampled may be more susceptible to granular disaggregation than the quartzite and gneiss samples in the Shackleton Range. These are still exceptionally low erosion rates by global standards but comparable to some of the rates measured in the Transantarctic Mountains (0.2–$1 \, m \, Ma^{-1}$, Summerfield et al. 1999), especially those of low relief, high altitude surfaces.

In the Shackleton Range and Ellsworth Mountains ice sheet expansion during the LGM caused thickening of < 340 m (Shackleton Range) or < 480 m (Ellsworth Mountains). In the Ellsworth Mountains the West Antarctic ice sheet thinned from this upper limit progressively through the Holocene (Bentley et al. 2010). In Forlidas valley the mid-Holocene ages of the higher shorelines present around Forlidas Pond show that the ice sheet had retreated from Forlidas and Davis valleys prior to the mid-Holocene. Our interpretation is that the bouldery moraines in northern Davis Valley therefore mark the LGM position and subsequent retreat of the ice sheet, representing only a 2.5–3 km maximum advance, to an altitude of 400 m which

is 216 m above the lowest part of the Davis Valley, but of similar altitude to the surface of the Ford Ice Piedmont *c.* 1 km north of the Davis Valley (Fig. 3). This suggests an ice advance into the valley occurred but did not involve any substantial thickening, perhaps consistent with this being an ablation area (Van den Broeke *et al.* 2006). An alternative would be that the drift sheets on the valley sides represent the LGM but this seems unlikely because it would imply a complex sequence of advance and retreat (Stages 4–7) during the glacial-interglacial transition, and such a pattern has not been observed at other better dated sites in the Transantarctic Mountains. Similar drift sheets occur in the north-western part of the Shackleton Range in the Haskard Highland and Mount Provender regions and predate the LGM (Höfle & Buggisch 1995, Fogwill *et al.* 2004). However, with the age constraints available we cannot precisely identify an LGM position of the ice sheet margin.

Although the other stages remain undated we can speculate by analogy to the McMurdo Dry Valleys that Stage 6 (advance and retreat of outlet glaciers) may date from a previous interglacial. Higgins *et al.* (2000) showed that interglacial advances of EAIS outlet glaciers have been a persistent feature of that sector of the EAIS inland of the McMurdo Dry Valleys, due to increased precipitation (inferred from the presence of large proglacial lakes) compared with glacial periods. This differs from outlet glaciers in the McMurdo Dry Valleys which are linked to the sea and responded to a fall in sea level and expanded during glacial periods. The Salle Snowfield probably responded more to precipitation change than to any sea level forcing that may have contributed to ice sheet change.

Being at the junction between the west and the east Antarctic ice sheets, constraining the ice history of the Dufek Massif, and the Weddell Sea embayment more generally, contributes to understanding long-term ice sheet history, and ice sheet contributions to sea level (Fogwill *et al.* 2004). In terms of the Miocene–Pleistocene evolution of the East Antarctic ice sheet the results presented here suggest a relatively stable ice sheet in this sector after Stage 1. Although ice expanded into the over-deepened valleys it did not reach altitudes substantially thicker than occurs today on the Ford Ice Piedmont within *c.* 1–2 km of the Davis Valley. The geomorphological evidence in the Dufek Massif certainly shows both ice sheet fluctuations and periods of deglaciation but these were of a relatively modest scale, unless non-erosive cold-based glaciation has been pervasive, but we have no field evidence to suggest such a complication. Our data constrained ice thickening to < 760 m altitude throughout the last > 1 Ma with LGM ice in the region representing only a 2–3 km advance to an altitude of 400 m with many of the upper slopes of the mountains remaining ice-free. This is consistent with an emerging dataset from around the Weddell Sea rim that imply only rather modest thickening at the LGM (Mulvaney *et al.* unpublished, Fogwill *et al.* 2004, Bentley *et al.* 2006,

2010, Hein *et al.* 2011). This implies a limited sea level contribution from areas between the major ice streams of this sector and supports initial analyses of an ice core drilled at Berkner Island which demonstrated that the ice rise forming the island remained a separate ice dispersal centre throughout the last glacial cycle and was not over-ridden (Mulvaney *et al.* unpublished). Further work is required to more fully constrain the glacial history, and to incorporate these data into robust ice sheet models of the Weddell Sea embayment.

Because the glacial geomorphology of this region holds such a rich record of ice sheet fluctuations more detailed study of the area could provide further insights into the history of the ice sheet around the Weddell Sea embayment, and complement understanding of the better studied sectors of the Transantarctic Mountains in the Ross Sea embayment, and elsewhere in East Antarctica (e.g. Moriwaki 1992, Mackintosh *et al.* 2007, Altmaier *et al.* 2010). Some obvious priorities for further work in the Dufek Massif would be: i) to attempt to date some of the older landscape-forming events (Stages 1 and 2) through detailed landform and soil development studies (cf. Bockheim 2002), ii) to use some combination of ^{3}He, ^{21}Ne and ^{36}Cl cosmogenic isotopes to date the bouldery moraines (Stage 7), and thus avoid the problem of re-working of Dover Sandstone erratics. Dating the mafic boulders stands a better chance of success because of the observation that these are emerging from the present-day ice margin and so at least some of them may thus possibly be free of inheritance, and iii) dating of depth profiles within drift using a suite of isotopes may provide constraints on some of the older deposits (Stages 3–6).

Conclusions

We have mapped the glacial geomorphology of two dry valleys in the northern Dufek Massif, and building on previous work, we propose a seven stage glacial history. From oldest to youngest these stages were:

- Alpine glaciation of the escarpment edge

- Over-riding warm-based glaciation

- Glacier advance to an upper limit (760 m)

- Two ice sheet advances to closely parallel limits in the valleys

- Advance of the plateau outlet glaciers (including Edge Glacier) to merge with the ice sheet

- Finally an advance and retreat of the main ice sheet margin of the Ford Ice Piedmont.

We have attempted to provide age constraints for some of these glacial events using paired cosmogenic ^{10}Be-^{26}Al exposure ages on erratic boulders, composed of Dover Sandstone. Some of these samples yield results implying continuous exposure without evidence of complex burial-exposure events. In the

case of our oldest mapped depositional feature (high level drift deposits marking Stage 3) the cosmogenic data provide a minimum age for the glacier advance (and the preceding events) of > 1.0 Ma. Analyses of samples from other depositional landforms lower down in Davis Valley have yielded complex exposure histories and we cannot precisely constrain the ages of these glacier and ice sheet advances. Radiocarbon dating shows that the most recent ice sheet advance and retreat must predate the mid-Holocene.

Our results therefore suggest only a minor LGM (or earlier) ice sheet advance and are consistent with an emerging dataset from around the Weddell Sea rim that imply only rather modest ice sheet thickening in this region at the LGM.

Acknowledgements

Supplemental material

Supplemental material describing laboratory procedures and calculations will be found at http://dx.doi.org/10.1017/S0954102012000016.

References

ALTMAIER, M., HERPERS, U., DELISLE, G., MERCHEL, S. & OTT, U. 2010. Glaciation history of Dronning Maud Land (Antarctica) reconstructed from *in situ* produced cosmogenic ^{10}Be, ^{26}Al, ^{21}Ne. *Polar Science*, **4**, 42–61.

AUGHENBAUGH, N., NEUBURG, H. & WALKER, P. 1958. *Ellsworth Station glaciological and geological data. Report 825-1-Part I, USNC-IGY Antarctic Glaciological Data Field Work 1957 and 1958*. Columbus, OH: Ohio State University Research Foundation.

BALCO, G., STONE, J., LIFTON, N. & DUNAI, T. 2008. A simple, internally consistent, and easily accessible means of calculating surface exposure ages and erosion rates from Be-10 and Al-26 measurements. *Quaternary Geochronology*, **3**, 174–195.

BASSETT, S.E., MILNE, G.A., BENTLEY, M.J. & HUYBRECHTS, P. 2007. Modelling Antarctic sea level data to explore the possibility of a dominant Antarctic contribution to meltwater pulse IA. *Quaternary Science Reviews*, **26**, 2113–2127.

BEHRENDT, J.C., HENDERSON, J.R., MEISTER, L. & RAMBO, W.K. 1974. Geophysical investigations of the Pensacola Mountains and adjacent glacierized areas of Antarctica. *United States Geological Survey, Professional Report*, **844**.

BENTLEY, M.J. 1999. Volume of Antarctic ice at the Last Glacial Maximum, and its impact on global sea level change. *Quaternary Science Reviews*, **18**, 1569–1595.

BENTLEY, M.J., FOGWILL, C.J., KUBIK, P.W. & SUGDEN, D.E. 2006. Geomorphological evidence and cosmogenic 10Be/26Al exposure ages for the Last Glacial Maximum and deglaciation of the Antarctic Peninsula ice sheet. *Geological Society of America Bulletin*, **118**, 1149–1159.

BENTLEY, M.J., FOGWILL, C.J., LE BROCQ, A.M., HUBBARD, A.L., SUGDEN, D.E., DUNAI, T. & FREEMAN, S.P.H.T. 2010. Deglacial history of the West Antarctic ice sheet in the Weddell Sea embayment: constraints on past ice volume change. *Geology*, **38**, 411–414.

BIERMAN, P.R., MARSELLA, K.A., PATTERSON, C., DAVIS, P.T. & CAFFEE, M. 1999. Mid-Pleistocene cosmogenic minimum-age limits for pre-Wisconsinan glacial surfaces in southwestern Minnestoa and southern Baffin Island: a multiple nuclide approach. *Geomorphology*, **27**, 25–39.

BOCKHEIM, J.G. 2002. Landform and soil development in the McMurdo Dry Valleys, Antarctica: a regional synthesis. *Arctic, Antarctic and Alpine Research*, **34**, 308–317.

BOYER, S.J. 1979. Glacial geological observations in the Dufek Massif and Forrestal Range, 1978-79. *Antarctic Journal of the United States*, **14**(5), 46–48.

CHMELEFF, J., VON BLANCKENBURG, F., KOSSERT, K. & JAKOB, D. 2010. Determination of the 10Be half-life by multicollector ICP-MS and liquid scintillation counting. *Nuclear Instruments and Methods in Physics Research, Section B: Beam Interactions with Materials and Atoms*, **268**, 192–199.

CLARK, P.U. & MIX, A.C. 2002. Ice sheets and sea level of the Last Glacial Maximum. *Quaternary Science Reviews*, **21**, 1–7.

CONWAY, H., HALL, B.L., DENTON, G.H., GADES, A.M. & WADDINGTON, E.M. 1999. Past and future grounding line retreat of the West Antarctic ice sheet. *Science*, **286**, 280–283.

DAVIS, C.H., LI, Y., MCCONNELL, J.R., FREY, M.M. & HANNA, E. 2005. Snowfall-driven growth in East Antarctic ice sheet mitigates recent sea level rise. *Science*, **308**, 1898–1901.

DENTON, G.H. & HUGHES, T.J. 2002. Reconstructing the Antarctic ice sheet at the Last Glacial Maximum. *Quaternary Science Reviews*, **21**, 193–202.

DENTON, G.H., ARMSTRONG, R.L. & STUIVER, M. 1971. The late Cenozoic glacial history of Antarctica. *In* TUREKIAN, K.K., *ed. The late Cenozoic glacial ages*. New Haven: Yale University Press, 267–306.

DENTON, G.H., BOCKHEIM, J.G., RUTFORD, R.H. & ANDERSEN, B.G. 1992. Glacial history of the Ellsworth Mountains, West Antarctica. *Geological Society of America Memoir*, **170**, 403–432.

EVANS, D.J.A., ed. 2003. *Glacial landsystems*. London: Arnold, 532 pp.

FERNANDEZ-CARAZO, R., HODGSON, D.A., CONVEY, P. & WILMOTTE, A. 2011. Low cyanobacterial diversity in biotopes of the Transantarctic Mountains (80–82°S), Antarctica. *FEMS Microbiology Ecology*, **77**, 503–517.

FERRIS, J., JOHNSON, A. & STOREY, B. 1998. Form and extent of the Dufek intrusion, Antarctica, from newly compiled aeromagnetic data. *Earth and Planetary Science Letters*, **154**, 185–202.

FOGWILL, C.J., BENTLEY, M.J., SUGDEN, D.E., KERR, A.R. & KUBIK, P.W. 2004. Cosmogenic nuclides ^{10}Be and ^{26}Al imply limited Antarctic ice sheet thickening and low erosion in the Shackleton Range for >1 m.y. *Geology*, **32**, 265–268.

FORD, A.B. 1976. Stratigraphy of the layered gabbroic Dufek intrusion, Antarctica: contributions to stratigraphy. *Geological Survey Bulletin 1405-D*, 36 pp.

FORD, A.B. 1990. The Dufek intrusion of Antarctica. *Antarctic Research Series*, **51**, 15–32.

FORD, A.B., SCHMIDT, D.L. & BOYD, W.W. 1978. *Geologic map of the Davis Valley quadrangle and part of the Cordiner Peaks quadrangle, Pensacola Mountains, Antarctica*. United States Antarctic Research Program, Map **A-10**, 1:250 000. Reston, VA: US Geological Survey.

GOSSE, J.C. & PHILLIPS, F.M. 2001. Terrestrial *in situ* cosmogenic nuclides: theory and application. *Quaternary Science Reviews*, **20**, 1475–1560.

HEIN, A.S., FOGWILL, C.J. SUGDEN, D.E. & XU, S. 2011. Glacial/interglacial ice-stream stability in the Weddell Sea embayment, Antarctica. *Earth and Planetary Science Letters*, **307**, 211–221.

HIGGINS, S.M., HENDY, C.H. & DENTON, G.H. 2000. Geochronology of Bonney drift, Taylor Valley, Antarctica: evidence for interglacial expansions of Taylor Glacier. *Geografiska Annaler*, **82A**, 391–409.

HODGSON, D.A., CONVEY, P., VERLEYEN, E., VYVERMAN, W., MCINTOSH, W., SANDS, C.J., FERNÁNDEZ-CARAZO, R., WILMOTTE, A., DE WEVER, A., PEETERS, K., TAVERNIER, I. & WILLEMS, A. 2010. The limnology and biology of the Dufek Massif, Transantarctic Mountains 82° South. *Polar Science*, **4**, 197–214.

HÖFLE, H.C. & BUGGISCH, W. 1995. Glacial geology and petrography of erratics in the Shackleton Range, Antarctica. *Polarforschung*, **63**, 183–201.

KERR, A. & HERMICHEN, W.D. 1999. Glacial modification of the Shackleton Range, Antarctica. *Terra Antartica*, **6**, 353–360.

KESSLER, M.A. & WERNER, B.T. 2003. Self-organization of sorted patterned ground. *Science*, **299**, 380–383.

KORSCHINEK, G., BERGMAIER, A., FAESTERMANN, T., GERSTMANN, U.C., KNIE, K., RUGEL, G., WALLNER, A., DILLMANN, I., VON GOSTOMSKI, L., KOSSERT, K., MAITI, M., POUTIVTSEV, M. & REMMERT, A. 2010. A new value for the half-life of 10Be by Heavy-Ion Elastic Recoil Detection and liquid scintillation counting. *Nuclear Instruments and Methods B*, **268**, 187.

LEWIS, A.R., MARCHANT, D.R., ASHWORTH, A.C., HEDENAS, L., HEMMING, S.R., JOHNSON, J.V., LENG, M.J., MACHLUS, M.L., NEWTON, A.E. & RAINE, J.I. 2008. Mid-Miocene cooling and the extinction of tundra in continental Antarctica. *Proceedings of the National Academy of Sciences of the United States of America*, **105**, 10 676–10 680.

MACKINTOSH, A., WHITE, D., FINK, D., GORE, D.B., PICKARD, J. & FANNING, P.C. 2007. Exposure ages from mountain dipsticks in Mac. Robertson Land, East Antarctica, indicate little change in ice sheet thickness since the Last Glacial Maximum. *Geology*, **35**, 551–554.

MORIWAKI, K. 1992. Late Cenozoic glacial history in the Sør-Rondane Mountains, East Antarctica. *In* YOSHIDA,Y., KAMINUMA, K. & SHIRAISHI, K., *eds. Recent progress in Antarctic earth science*. Tokyo: Terra Scientific, 661–667.

NISHIIZUMI, K. 2004. Preparation of 26Al standards. *Nuclear Instruments and Methods in Physics Research B*, **223**, 388–392.

NISHIIZUMI, K., WINTERER, E.L., KOHL, C.P., KLEIN, J., MIDDLETON, R., LAL, D. & ARNOLD, J.R. 2007. Absolute calibration of Be-10 AMS standards. *Nuclear Instruments and Methods in Physics Research B*, **258**, 403–413.

PEETERS, K., HODGSON, D.A., CONVEY, P. & WILLEMS, A. 2011a. Culturable diversity of heterotrophic bacteria in Forlidas Pond (Pensacola Mountains) and Lundström Lake (Shackleton Range), Antarctica. *Microbial Ecology*, **62**, 399–413.

PEETERS, K., VERLEYEN, E., HODGSON, D.A., CONVEY, P., ERTZ, D., VYVERMAN, W. & WILLEMS, A. 2011b. Heterotrophic bacterial diversity in aquatic microbial mat communities from Antarctica. *Polar Biology*, 10.1007/s00300-00011-01100-00304.

SHEVENELL, A.E., KENNETT, J.P. & LEA, D.W. 2004. Middle Miocene Southern Ocean cooling and Antarctic cryosphere expansion. *Science*, **305**, 1766–1770.

STONE, J.O., BALCO, G.A., SUGDEN, D.E., CAFFEE, M.W., SASS, L.C., COWDERY, S.G. & SIDDOWAY, C. 2003. Holocene deglaciation of Marie Byrd Land, West Antarctica. *Science*, **299**, 99–102.

SUMMERFIELD, M.A., STUART, F.M., COCKBURN, H.A.P., SUGDEN, D.E., DENTON, G.H., DUNAI, T. & MARCHANT, D.R. 1999. Long-term rates of denudation in the Dry Valleys, Transantarctic Mountains, southern Victoria Land, Antarctica, based on *in-situ*-produced cosmogenic ^{21}Ne. *Geomorphology*, **27**, 113–129.

VAN DEN BROEKE, M., VAN DE BERG, W.J., VAN MEIJGAARD, E. & REIJMER, C. 2006. Identification of Antarctic ablation areas using a regional atmospheric climate model. *Journal of Geophysical Research*, 10.1029/2006JD007127.

VAN LIPZIG, N.P.M., TURNER, J., COLWELL, S.R. & VAN DEN BROEKE, M.R. 2004. The near-surface wind field over the Antarctic continent. *International Journal of Climatology*, **24**, 1973–1982.